https://doi.org/10.48048/tis.2022.5686

Investigation of Optical, Structural, Morphological and Electrical Properties of Electrodeposited Cobalt Doped Copper Selenide ($Cu_{1-x}Co_xSe$) Thin Films

Nonso Livinus Okoli[1,2,*], Laz Nnadozie Ezenwaka[2], Ngozi Agatha Okereke[2], Ifeyinwa Amaka Ezenwa[2] and Nwode Augustine Nwori[2]

[1]*Department of Physics, Legacy University Okija, Okija, Nigeria*
[2]*Department of Industrial Physics, Chukwuemeka Odumegwu Ojukwu University, Igbariam, Nigeria*

([*]Corresponding author's e-mail: okolinonsolivinus@gmail.com, okoli.nl@legacyuniversity.edu.ng)

Received: 9 May 2021, Revised: 18 June 2021, Accepted: 25 June 2021

Abstract

Undoped and cobalt doped copper selenide thin films have been successfully prepared unto fluorine tin oxide (FTO) substrates by electrodeposition method using copper acetate, cobalt nitrate and selenium (IV) oxide as precursors for copper, cobalt and selenium ions respectively. Deposited thin films were subjected to optical, structural, morphological, compositional and electrical analysis using spectrophotometer, x-ray diffractometer, scanning electron microscope (SEM), energy dispersive x-ray spectroscopy (EDS) and 4-point probe. Optical results observed between the wavelength range of 300 nm and 1,000 nm showed that the films have good optical responses. Absorbance values ranged between 0.1 and 0.81 while transmittance lies between 15.59 and 78.68 %. Energy band gap of the films was found to vary from 2.10 to 2.28 eV. These results showed that cobalt as a dopant could be used to modify properties of copper selenide thin films. Structural analysis showed that the deposited films are polycrystalline in nature with hexagonal structural phase. Crystallite sizes of range 27.56 to 34.27 nm were obtained while dislocation density lied between 1.59×10^{15} and $1.05 \times 10^{15}\ lines/m^2$. Microstrain ranged between 1.39×10^{-3} and 1.13×10^{-3}. Micrograph images showed flake-like particles that increased in size as percentage of cobalt increased. Energy dispersive spectroscope (EDS) results confirmed the incorporation of cobalt on the deposited copper selenide films. Electrical resistivity of the films increased from 5.84×10^{-4} to $31.96 \times 10^{-4}\ \Omega\ cm$ while conductivity decreased from 17.11×10^2 to 3.13×10^2 S/cm as a result of variation in cobalt ion concentration. These properties of the deposited thin films positioned them for solar cell and optoelectronics device applications.

Keywords: Copper selenide, Cobalt dopant, XRD, Electrical properties, Semiconductor films

Introduction

Copper selenide is among the widely studied binary transition metal chalcogenide semiconducting materials. Copper selenide as a semiconducting material has a p-type conductivity due to copper vacancies with both direct and indirect band gap [1], a property which is found most useful in the solar cell production [2]. It exists in different stoichiometric composition such as CuSe (klockmannite), $CuSe_2$ (marcasite), Cu_2Se (bellidoite), Cu_3Se_2 (umagnite) Cu_5Se_4 (athabaskite) and non-stoichiometric composition $Cu_{2-x}Se$ (berzelianite) [3-5]. Copper selenide occurs in broadly different crystallographic phases even at room temperature. This includes cubic, hexagonal, orthorhombic, monoclinic and tetragonal. Their formation depend upon method of preparation [6,7] and growth conditions. Reports have shown that CuSe mostly possessed hexagonal structural phase at room temperature and go through phase transition to orthorhombic at 48 °C and back to hexagonal phase at 120 °C. If exposed to high temperatures, copper selenide decomposes into $Cu_{2-x}Se$ and selenium. Energy band gap of CuSe thin films has been shown by many researchers to vary depending on the fabrication methods and growth parameters. CuSe shows a direct band gap of 2. 2 eV and an indirect bandwidth of 1.4 eV [8]. Many researchers have deposited copper selenide thin films using different methods such as chemical bath method [9,10], electrodeposition [11,12], spray pyrolysis [2,4,13], spin coating [13,14], SILAR method [13-15].

Cobalt ion has served as a dopant atom to ZnSe [16,17], CdSe [18], Bi_2Se_3 [19], NiSe [20]. Results obtained from these works showed that cobalt as a dopant has the tendency to modify optical, structural, electrical, morphological, compositional and magnetic properties of the parent binary metal selenide thin films. No literature works were recorded for doping copper selenide thin film with cobalt and this formed the motivation for this work. In this work, thin films of undoped and cobalt doped copper selenide were deposited using electrodeposition method. The electrodeposition setup is a 3-electrodes configuration system containing working electrode, counter electrode and reference electrode as shown in **Figure 1**.

Materials and methods

Three-electrodes (3-Es) electrodeposition configuration was employed for the synthesis of undoped and cobalt doped copper selenide thin films on conducting substrate (FTO). The experimental set up containing the electrolyte, power supply unit and the 3 electrodes is shown in **Figure 1** below. The conducting substrate (FTO) was used as the working electrode (cathode). Platinum electrode served as the counter electrode (anode). The reference electrode used is a Silver/Silver chloride electrode (Ag/AgCl). Dazheng digital DC-power supply unit (model: PS-1502A) was used as source of energy supply to the electrodeposition setup. Two digital multimeters, (DT9201A CE and Mastech: MY60) were used in the setup for measuring voltage and current respectively.

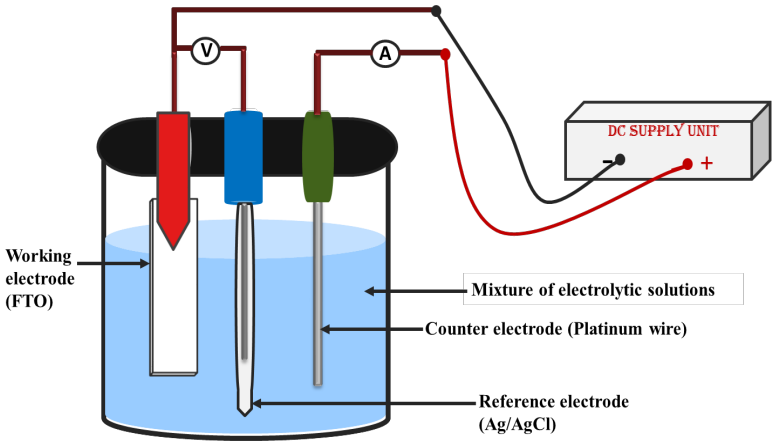

Figure 1 Schematic diagram of the 3-electrodes (3-Es) Electrodeposition set-up.

For deposition of copper selenide thin film, the aqueous electrolytic bath composed of 15 mL of 0.25 M Copper acetate and 15 mL of 0.2 M selenium dioxide were prepared and magnetically stirred for 5 min. The solution was mixed with 5 mL of 0.05 M $NaSO_4$ which served as a supporting electrolyte and 5 mL of 0.1 M H_2SO_4 that served as a pH adjuster. The final solution was stirred for 5 min. The 3 electrodes were immersed into the bath containing the electrolytic solution and 2 volts was maintained in the setup for 40 s. For the deposition of Co doped CuSe thin films, doping formulation according to [21] was adopted. Dopant percentage of 2, 4, 6 and 8 % was used. Similar procedure used for deposition of copper selenide thin film was adopted but with different concentrations of Co ion and Cu ion precursors as shown in **Table 1**. Four samples with different dopant percentages were fabricated.

Table 1 Bath parameter of Co ion optimization of $Cu_{1-x}Co_xSe$ thin film.

Cu ion precursor		**Co ion precursor**		**0.2 M SeO_2**	**0.05 M Na_2SO_4**	**0.1 M H_2SO_4**	**Voltage**	**Time**
Con. (mole)	Vol. (mL)	Con. (mole)	Vol. (mL)	Vol. (mL)	Vol. (mL)	Vol. (m:)	(volts)	(sec.)
0.250	15.00	-	-	15.00	5.00	5.00	2.00	40.0
0.245	15.00	0.005	15.00	15.00	5.00	5.00	2.00	40.0
0.240	15.00	0.010	15.00	15.00	5.00	5.00	2.00	40.0
0.235	15.00	0.015	15.00	15.00	5.00	5.00	2.00	40.0
0.230	15.00	0.020	15.00	15.00	5.00	5.00	2.00	40.0

Electrosynthesized thin films were subjected to structural, optical, morphological, compositional and electrical studies. Optical study was carried out using 756S UV-VIS spectrophotometer. Structural analysis of the films were obtained using Empyrean XRD diffractometer. Morphology and compositional analysis were carried out using Nova NanoSEM and MIRA TESCAN SEM machine while electrical properties of the films were analyzed using Keithley 2,400-LV source meter.

Results and discussion

Film thickness measurement

The deposited film thicknesses (t) were evaluated using the gravimetric method given by [22,23];

$$d = \frac{\Delta m}{\rho A}, \quad (1)$$

where Δm is the mass of the film. A is the surface area of the deposited film and ρ is the bulk density of the material film. The masses of the deposited films were obtained by finding the difference in mass between the mass of the glass substrate and the film after deposited and the mass of glass substrate before deposition.

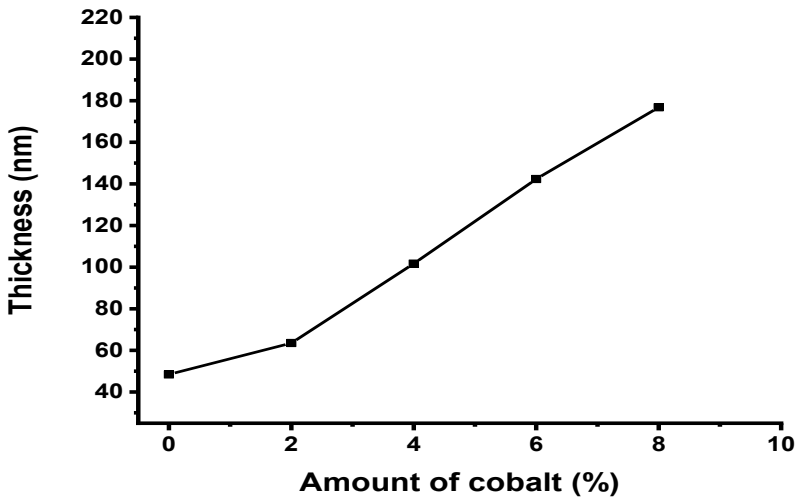

Figure 2 Graph of thickness against amount of cobalt ion.

Figure 2 showed the plot of thickness against amount of Co^{2+} ion. The result showed that as the Co^{2+} percentage increased, the thickness of the films increased. The deposited films are observed to be adhesive and uniform. CuSe film has the least thickness of 48.41 nm and the thickness was found to increase as cobalt ions were incorporated into copper selenide structure. The thickness increased to a peak value of 176.79 nm. The increase in film thickness as percentage of Co^{2+} ion increases could be explained on the basis of ions concentration in the electrolyte and film formation. When a few percentages of Cobalt dopant atoms are added into the reaction bath, the electrolyte ions concentration slightly increased thereby resulting to increase in the film growth rate [24,25]. Due to the fact that Co^{2+} ions are relatively small compared to the Cu^{2+}, they can easily serve as substitutional impurities that can occupy the sites of the host lattice (Cu^{2+}). The substitutional entrance of Co^{2+} dopant ions with slightly larger ionic radii (~ 7.5 Å) than that of Cu^{2+} (~ 0.73) leads to expansion of the host lattice and hence lead to particle size increase as well as increase in the film thickness.

Structural analysis

Crystal structural analyses were done using X-ray diffractometer machine. From the X-ray diffraction pattern obtained, other structural properties such as d-spacing, full width at half maximum (FWHM) were obtained. The crystallite sizes (D) and micro-strain of the films were evaluated using Scherrer's formula as given in Eq. (2). Debye-Scherrer's formula for calculating crystallite sizes of a thin film material is given by [26,27] as;

$$D = \frac{0.9\,\lambda}{\beta \cos\theta} \tag{2}$$

Where β is the full width at half maximum of the diffraction angles, λ is the wavelength of Cu-kα1 radiation used for X-ray diffraction analysis and θ is the diffraction angle. The dislocation density (δ) of thin films can be estimated using expression as provided by [28,29] in Eq. (3);

$$\delta = \frac{1}{D^2}. \tag{3}$$

Micro-strain (ε) of thin film sample can be estimated using the expression in Eq. (4) as given by [29,30];

$$\varepsilon = \frac{\beta}{4\tan\theta} \tag{4}$$

Figure 3 shows the X-ray diffraction patterns of copper selenide and cobalt doped copper selenide thin films. The X-ray diffraction results show that the undoped and doped copper selenide films have phase of copper selenide. Structural parameters of the deposited thin films are presented in **Table 2**. All the peaks correspond to the peaks present in the standard Powder Diffraction File (PDF) card number 00-020-1020 of JCPDS-ICDD (The Joint Committee on Powder Diffraction Standard - International Centre for Diffraction Data). Similar structure for copper selenide thin films has been obtained by [6,31]. No peaks corresponding to starting materials such as Cu ion and Co ion precursors or their other selenide phases were found in the pattern. This purely revealed that doping CuSe with Co^{2+} ion does not affect the crystal structure of CuSe. The matching of the calculated d_{hkl} values and the standard ones confirms that all the deposited films crystallize well in the hexagonal structure with preferential orientation of the crystallites along the (110) direction with 2 theta angles of 46.075, 46.101, 46.127, 46.153 and 46.180 ° for undoped and cobalt doped copper selenide thin films.

Increase in dopant concentration caused an increase in intensity of the diffraction peaks and shift in the peaks towards larger angles as can be observed in **Table 2**. Peak shift towards higher angles as percentage of cobalt ion increases could be due to the fact that Co^{2+} atoms can comfortably occupy Cu^{2+} sites. This substitutional occupation of Cu^{2+} (ionic radius 0.73 Å) sites by Co^{2+} (ionic radius 0.75 Å) caused peak shift towards higher angles due to expansion of the lattice constant of the main ion (Cu^{2+}). Average crystallite sizes of the films deposited range from 27.56 to 34.27 nm. **Figure 4** showed the variation of crystallite size and dislocation density with percentage of dopant (Co^{2+} ion). Crystallite size of the films were found to increase while dislocation density decreases as percentage of cobalt increases. The observed variations in crystallite size, dislocation density and micro-strain was as a result of the fact that atomic radius of cobalt ion is slightly higher than that of copper ion. Also, values of micro-strain of the films were found to decrease as percentage of dopant increases. The changes in the crystallite size, dislocation density and micro-strain could be attributed to improvement in the crystal structure due to doping with cobalt ion.

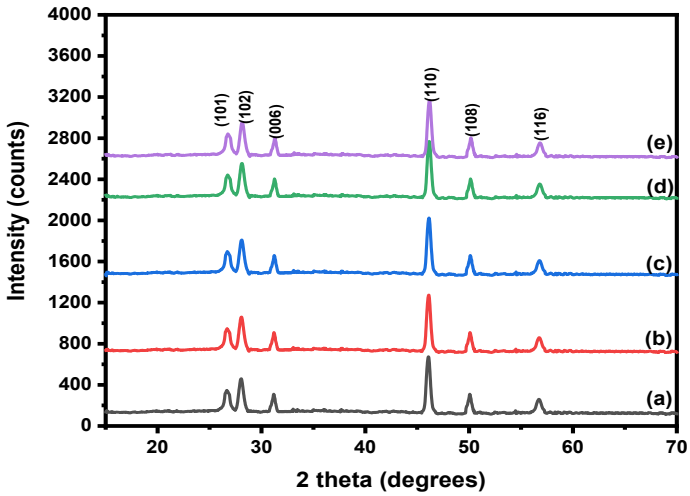

Figure 3 XRD pattern of cobalt doped copper selenide thin film (a) CuSe, (b) copper selenide doped with 2 % of cobalt ion, (c) copper selenide doped with 4 % of cobalt ion, (d) copper selenide doped with 6 % of cobalt ion and (e) copper selenide doped with 8 % of cobalt ion.

Table 2 Structural parameters of cobalt doped copper selenide thin films at varying concentration of cobalt ions.

Samples	2θ (°)		d-spacing (nm)		FWHM (°)	D (nm)	δ x 10^{15} (lines/m^2)	ε x 10^{-3}
	Std.	Obs.	Std.	Obs.				
CuSe	26.587	26.697	0.335	0.334	0.491	17.37	3.32	2.08
	28.127	28.049	0.317	0.318	0.363	23.57	1.8	1.54
	31.138	31.173	0.287	0.287	0.258	33.42	0.9	1.08
	46.085	46.075	0.197	0.197	0.288	31.36	1.02	1.15
	50.079	50.057	0.182	0.182	0.268	34.22	0.85	1.06
	56.707	56.721	0.162	0.162	0.371	25.41	1.55	1.42
			Average			**27.56**	**1.57**	**1.39**
Co: 2 %	26.587	26.723	0.335	0.333	0.461	18.49	2.93	1.96
	28.127	28.075	0.317	0.318	0.352	24.31	1.69	1.49
	31.138	31.199	0.287	0.286	0.218	39.55	0.64	0.92
	46.085	46.101	0.197	0.197	0.228	39.63	0.64	0.91
	50.079	50.083	0.182	0.182	0.208	44.10	0.51	0.82
	56.707	56.748	0.162	0.162	0.351	26.85	1.39	1.35
			Average			**32.16**	**1.45**	**1.32**
Co: 4 %	26.587	26.75	0.335	0.333	0.441	19.32	2.68	1.87
	28.127	28.101	0.317	0.317	0.322	26.58	1.42	1.36
	31.138	31.225	0.287	0.286	0.218	39.54	0.64	0.92
	46.085	46.127	0.197	0.197	0.238	37.96	0.69	0.95
	50.079	50.11	0.182	0.182	0.208	44.1	0.51	0.82
	56.707	56.774	0.162	0.162	0.311	30.3	1.09	1.19
			Average			**32.97**	**1.17**	**1.19**
Co: 6 %	26.587	26.776	0.335	0.333	0.431	19.78	2.56	1.83
	28.127	28.127	0.317	0.317	0.312	27.45	1.33	1.32
	31.138	31.251	0.287	0.286	0.228	37.84	0.7	0.96
	46.085	46.153	0.197	0.197	0.208	43.47	0.53	0.83
	50.079	50.136	0.182	0.182	0.208	44.13	0.51	0.82
	56.707	56.8	0.162	0.162	0.321	29.39	1.16	1.23
			Average			**33.68**	**1.13**	**1.17**
Co: 8 %	26.587	26.802	0.335	0.332	0.411	20.75	2.32	1.75
	28.127	28.153	0.317	0.317	0.302	28.36	1.24	1.28
	31.138	31.278	0.287	0.286	0.218	39.58	0.64	0.91
	46.085	46.180	0.197	0.196	0.218	41.47	0.58	0.87
	50.079	50.162	0.182	0.182	0.208	44.14	0.51	0.82
	56.707	56.827	0.162	0.162	0.301	31.34	1.02	1.16
			Average			**34.27**	**1.05**	**1.13**

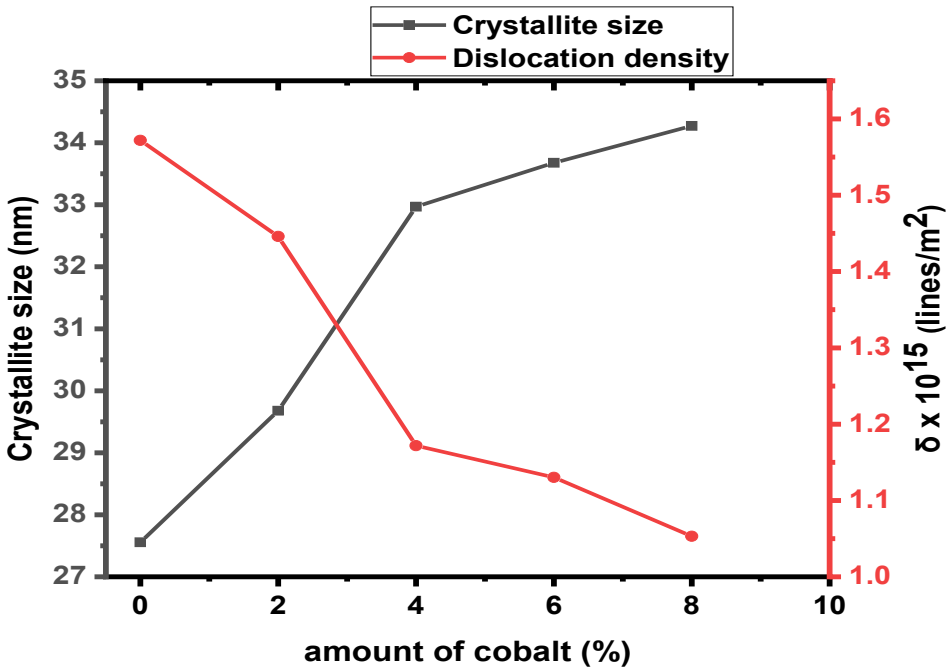

Figure 4 Variation of crystallite sizes and dislocation density with cobalt concentration.

Optical properties

Transmittance (T) of the film was evaluated using Eq. (5) as given by [32,33];

$$T = 10^{-A} \tag{5}$$

Reflectance (R) was obtained using the expression in Eq. (6) as given by [34,35];

$$R = 1 - [T \cdot \exp(A)]^{\frac{1}{2}} \tag{6}$$

The absorption coefficient (α) was calculated from the transmittance values using the Eq. (7) as given by [36,37];

$$\alpha = \frac{1}{t} \mathrm{In}\left(\frac{1}{T}\right). \tag{7}$$

Where t is film thickness obtained using Eq. (1). Extinction coefficient (k) was obtained using Eq. (8) as given by [38,39];

$$\mathrm{k} = \frac{\alpha\lambda}{4\pi} \tag{8}$$

Refractive index (η) of the films were calculated using Eq. (9) as given by [40,41];

$$\eta = \frac{1+R}{1-R} + \sqrt{\frac{4R}{(1-R)^2} - k^2} \tag{9}$$

Optical conductivity (σ_o) was estimated using Eq. (10) as given by [42,43];

$$\sigma_o = \frac{\alpha\eta c}{4\pi}. \tag{10}$$

Where c is the speed of light.

The energy band gap (E_g) was estimated using Tauc's model of Eq. (11) as given by [44,45];

$$(\alpha hv)^n = \beta(hv - E_g). \quad (11)$$

Where β is a constant, $n = 2$ for direct band gap. The energy band gaps of the films were obtained by extrapolating the straight portion of the plot of $(\alpha hv)^2$ against the photon energy (hv) at $(\alpha hv)^2 = 0$.

Figure 5 shows the graph of absorbance of deposited undoped and cobalt doped copper selenide thin films plotted against wavelength. The results showed that absorbance values decreased as wavelength of photon increases within UV and VIS regions but increased slightly within NIR region. Absorbance was also found to increase as percentage of cobalt increases. The increase in absorption of photon energy is an evidence that there is substitution of copper ions by cobalt ions in the lattice structure of copper selenide. Absorbance values observed for copper selenide thin film doped with various percentages of cobalt ions positioned them as potential materials for absorber layer of a thin film solar cell. Similar decrease in absorbance when cobalt was used as dopant atom had been obtained by [46,47].

Figure 6 shows the graph of transmittance of undoped and cobalt doped copper selenide thin films plotted against wavelength. Transmittance values of the films were found to increase as wavelength increases within UV and VIS regions. Slight decrease in transmittance values was observed in NIR region. Also, transmittance values were found to decrease as percentage of cobalt ion increases. This decrease in transmittance is as a result of high absorption of photon energy by the films occasioned by incorporation of cobalt ions within the lattices of copper selenide structure. Sahebi *et al.* [48] and Poongodi *et al.* [49] obtained similar trend in the transmittance of binary thin films of CdSe and ZnO doped with Ag and Co respectively.

Figure 7 shows the graph of reflectance of undoped and cobalt doped copper selenide thin films plotted against wavelength. Generally, the undoped and cobalt doped copper selenide thin films possessed low reflectance in all region of photon wavelength. The reflectance of the thin films increase from its least values within UV region to peak values of 20.20 and 20.33 % at 320 nm for undoped CuSe and CuSe doped with 2 % of cobalt ion, and 20.34 % at 335, 380 and 450 nm for films doped with 4, 6 and 8 % cobalt ion respectively. The reflectance values were found to decrease as wavelength increases within VIS region but later increase with increase in wavelength within NIR region. Also, reflectance values of the films were found to increase as cobalt ion concentration increases mostly within VIS region except for film doped with 4 % of the dopant. This results showed that these films are good absorber of photon energy within the visible region and could be used to shed UV radiation and for antireflective coatings.

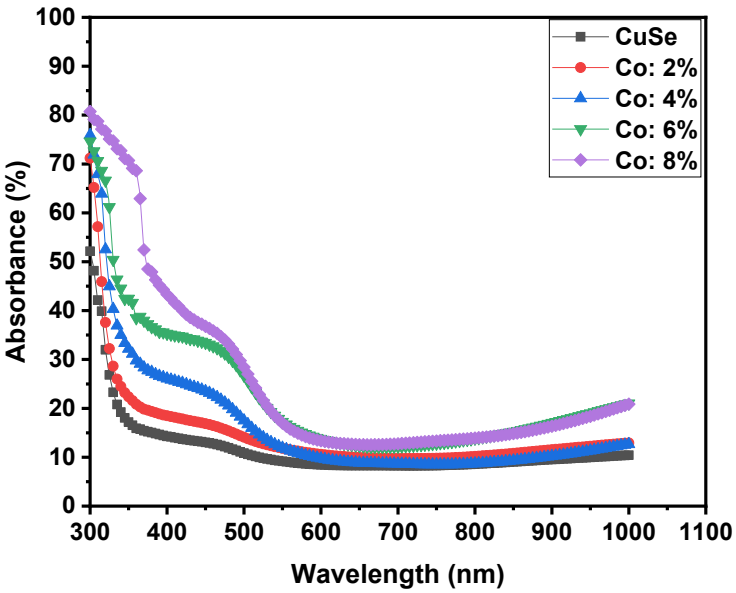

Figure 5 Plot of absorbance against wavelength for cobalt doped copper selenide thin films deposited at different percentage of cobalt ion.

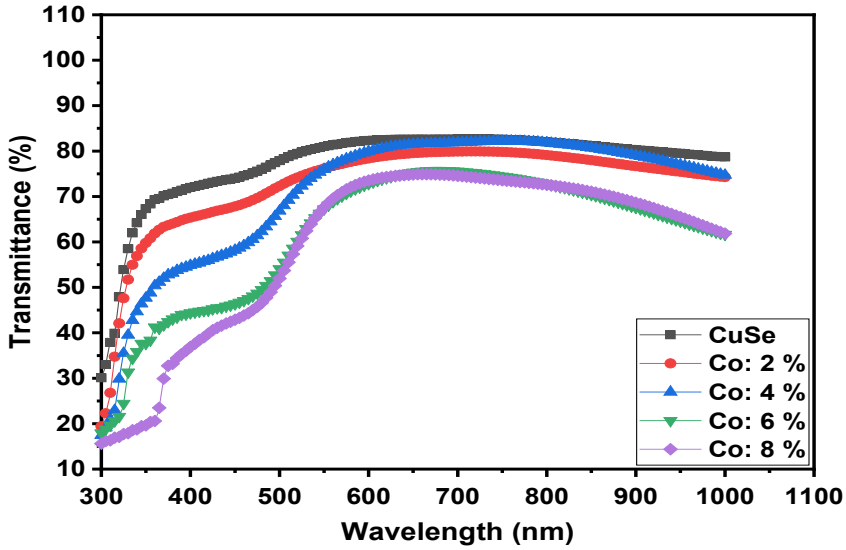

Figure 6 Plot of transmittance against wavelength for cobalt doped copper selenide thin films deposited at different percentage of cobalt ion.

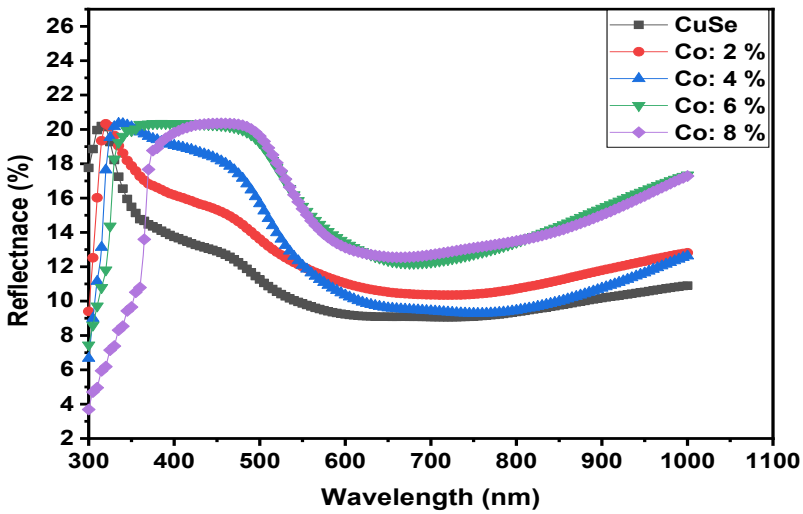

Figure 7 Plot of reflectance against wavelength for cobalt doped copper selenide thin films deposited at different percentage of cobalt ion.

Figure 8 shows the graph of extinction coefficient of undoped and cobalt doped copper selenide thin films at varying doping concentration. Extinction coefficient being the measure of the loss of photon energy due to absorption or scattering as it passes through the thin film materials was found to decrease within UV and VIS regions but increases toward NIR region. Extinction coefficient of the films was found to decrease as percentage of cobalt ion increase. Values of the extinction coefficient for the undoped and doped copper selenide thin film ranged between 0.10 and 0.62. These range of extinction coefficient values confirmed the photon absorption potentials of undoped and cobalt doped copper selenide thin films doped with different percentage of cobalt ion.

Figure 9 shows the graph of refractive index of undoped and cobalt doped copper selenide thin films plotted against wavelength. Undoped and cobalt doped copper selenide thin films possessed refractive index values that vary with photon wavelength. The refractive index of the thin films increase from it least values within UV region to peak values of 2.56 and 2.59 at 320 nm for undoped CuSe and CuSe doped with 2 % of cobalt ion, and 2.63 at 335, 380 and 450 nm for films doped with 4, 6 and 8 %

cobalt ion concentration respectively. The refractive index values were found to decrease as wavelength increases within VIS region but later increase with increase in wavelength within NIR region.

Figure 10 shows the graph of optical conductivity of undoped and cobalt doped copper selenide thin film plotted against wavelength. The result showed that optical conductivity of the deposited thin films decreased as wavelength increases within UV and VIS regions but increase slightly towards NIR region. Also, minor decrease in optical conductivity was observed as cobalt ion percentage increased in the deposited thin films.

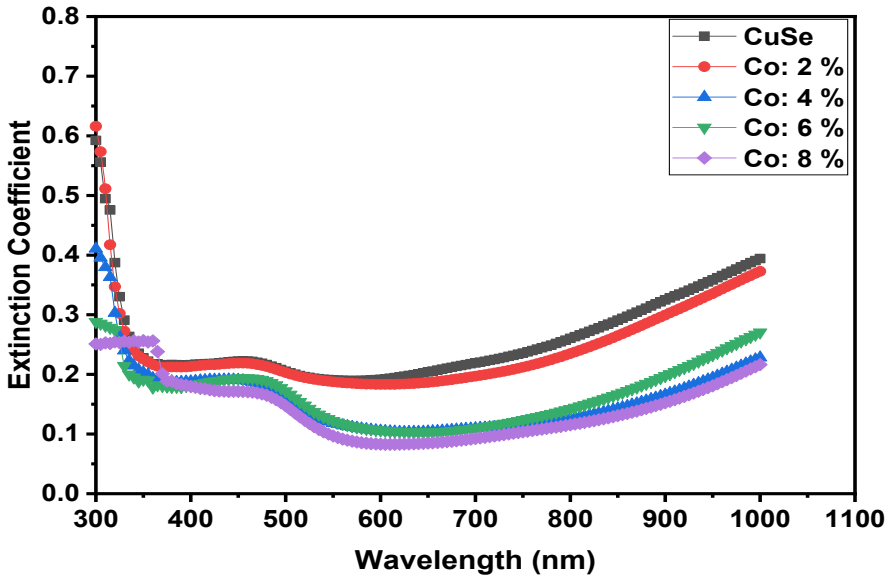

Figure 8 Plot of extinction coefficient against wavelength for cobalt doped copper selenide thin films deposited at different percentage cobalt ion.

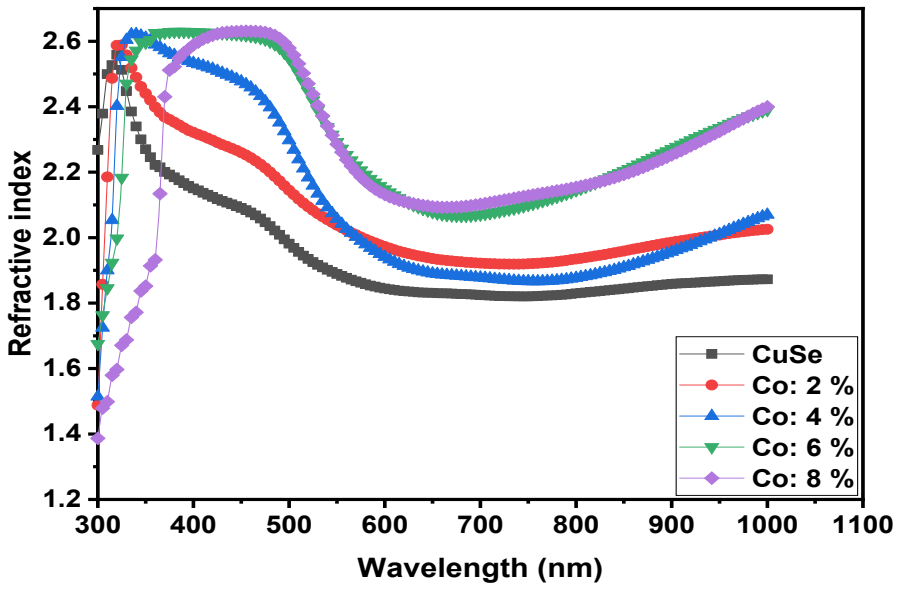

Figure 9 Plot of refractive index against wavelength for cobalt doped copper selenide thin films deposited at different percentage of cobalt ion.

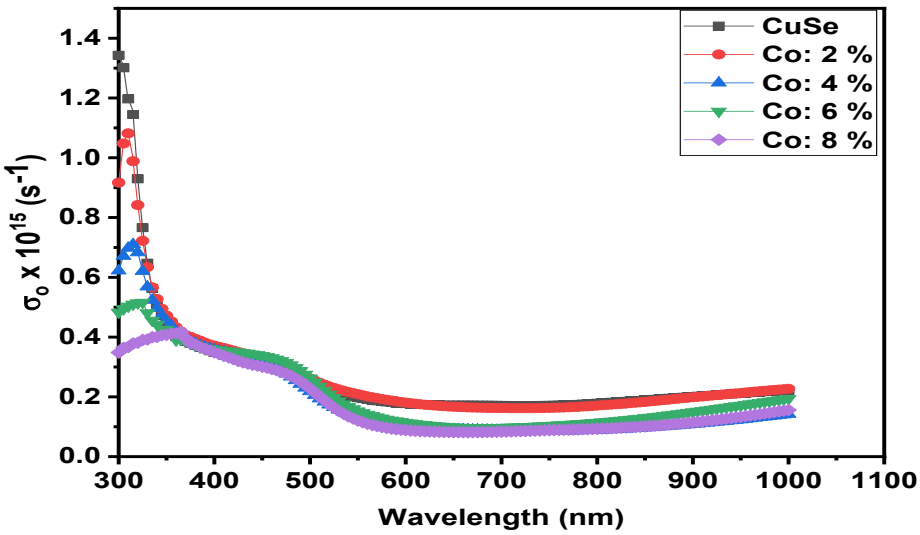

Figure 10 Plot of optical conductivity against wavelength for cobalt doped copper selenide thin films deposited at different percentage of cobalt ion.

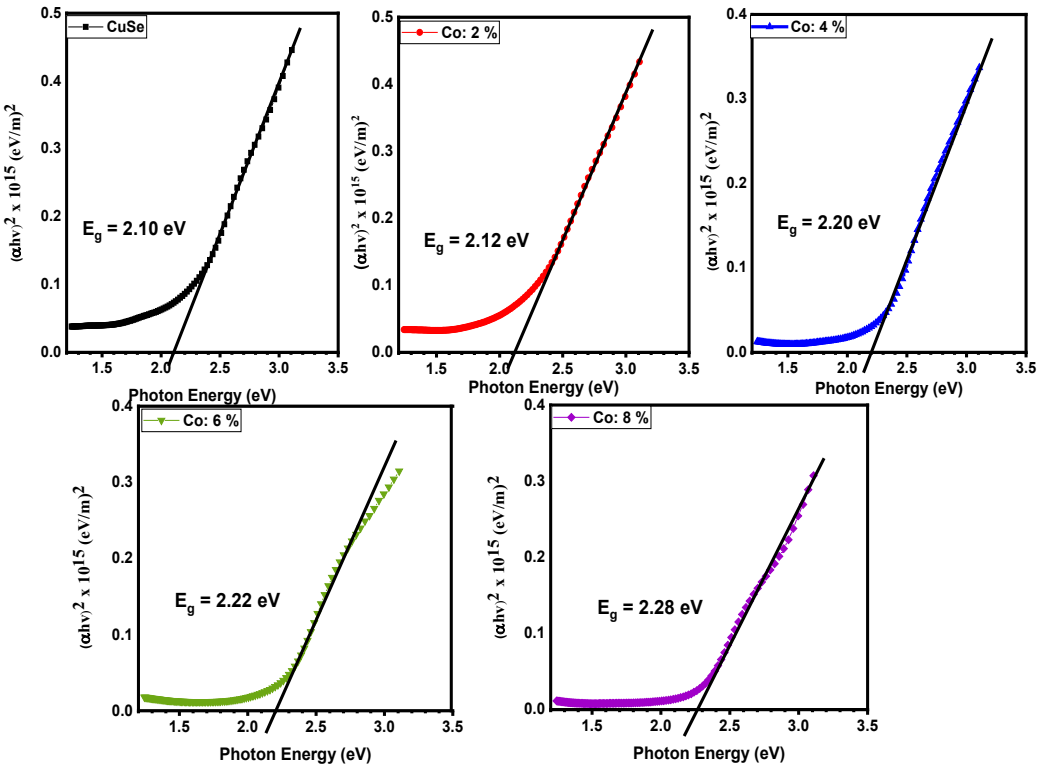

Figure 11 Plot of $(\alpha hv)^2$ against photon energy for cobalt doped copper selenide thin films deposited at different dopant concentrations.

Figure 11 shows the plot of $(\alpha hv)^2$ against photon energy for undoped and cobalt doped copper selenide thin films. From the plot, energy band gap of the films were estimated by extrapolation of the straight portion of the graph along the photon energy axis where $(\alpha hv)^2 = 0$. Energy band gap of 2.10 eV was obtained for undoped copper selenide thin film and the 2.12 eV obtained for CuSe doped with 2 % of cobalt ion. Energy band gap of 2.20, 2.22 and 2.28 eV were obtained for copper selenide thin films doped with 4, 6 and 8 % of cobalt ion concentration. The result revealed an increment in energy band gap

of films as cobalt ion concentration increases and confirms the possibility of band gap engineering of copper selenide using cobalt ion as impurity atoms. Similar trend in increase in band gap as percentage of dopant increases had been reported by [50-52]. This increment in energy band gap values could be related to cobalt ion incorporation in the structure of copper selenide and possibly be attributed to the quantum confinement effect of electron and hole in the deposited thin films.

Morphological/compositional analysis

Figure 12 shows the SEM images of undoped and cobalt doped copper selenide thin films deposited at different concentration of cobalt ions. The SEM images showed irregular flake-like particles that increase in size as percentage of cobalt increases. These particles are of unequal size distribution which suggest formation of polycrystalline thin films of copper selenide and cobalt doped copper selenide thin films as confirmed by XRD results. **Figure 13** showed the corresponding EDS results. The results confirmed the present of cobalt ion in increasing proportion as percentage of cobalt ion increases. These results showed that cobalt ions were effectively distributed into CuSe crystal structure which lead to improvements in the properties of CuSe thin films. Peaks corresponding to other elements such as tin (Sn), sulphur (S), oxygen (O), carbon (C) and nitrogen (N) were observed. Their presence is likely due to composition of substrates or precursor solutions used. **Table 3** shows the atomic percentages of the elements present in the deposited undoped and cobalt doped copper selenide thin films.

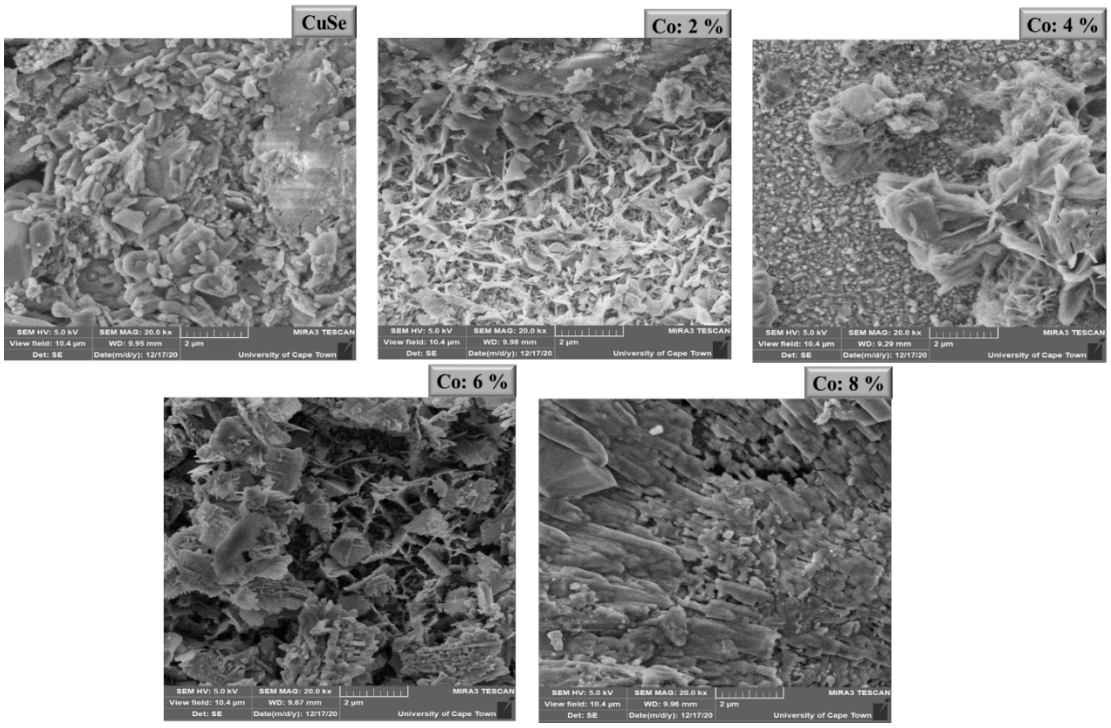

Figure 12 SEM Micrograph of undoped and Cobalt doped Copper Selenide Thin films.

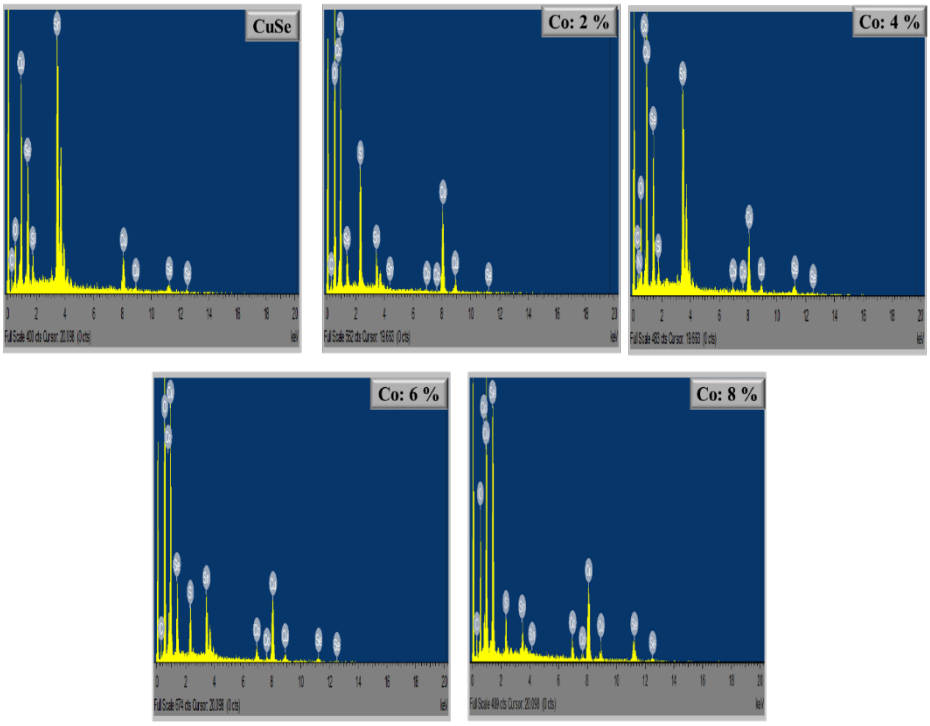

Figure 13 EDS Results of undoped and Cobalt doped Copper Selenide thin films.

Table 3 Elemental composition of deposited undoped and Cobalt doped Copper selenide thin films.

Samples	C	O	S	Si	Co	Cu	Se	Sn	Total
					(%)				
CuSe	6.92	19.45	-	1.11	-	30.46	19.59	22.47	100
Co: 2 %	6.24	15.00	-	0.08	1.57	37.69	22.67	16.75	100
Co: 4 %	6.35	14.41	-	1.24	1.93	41.75	18.62	15.70	100
Co: 6 %	4.72	13.33	-	2.70	2.57	44.84	20.29	11.55	100
Co: 8 %	6.20	10.95	2.01	-	3.47	46.14	22.90	8.33	100

Electrical properties

The measurement of dc conductivities was accomplished through the 4-point probe technique The 4-point probe apparatus has 4 probes in a straight line with an equal inter-probing spacing. A constant current passes through 2 outer probes and an output voltage is measured across the 2 inner probes. The 4 point probe machine gives the values of the resistance (V/I), current and voltage of the films while the electrical conductivities and resistivity of the synthesized thin film were determined using expressions as given by [53-56] in Eqs. (12) and (13) respectively;

$$\rho = \frac{\pi t}{ln\,2}\left(\frac{V}{I}\right) = 4.523t\left(\frac{V}{I}\right), \tag{12}$$

and electrical conductivity is given as;

$$\sigma = \frac{1}{\rho} \tag{13}$$

where t is the thickness of the films obtained using Eq. (1)

Electrical properties of cobalt doped copper selenide thin film synthesized at different cobalt ion concentration is shown in **Table 4**. The result revealed a variation in the electrical properties due to the doping of CuSe with cobalt ion. Electrical resistivity of $5.84 \times 10^{-4}\ \Omega\ cm$ and conductivity of $17.11 \times 10^{2}\ (S/cm)$ were obtained for CuSe thin film. These values correspond to results obtained by [57,58]. On doping CuSe with cobalt ion, the resistivity of the films was found to increase to $31.96 \times 10^{-4}\ (\Omega\ cm)$ while the electrical conductivity decreased to $3.13 \times 10^{2}\ (S/cm)$ as doping concentration increases. Helan *et al*. [59] obtained similar increase in electrical resistivity when copper selenide was doped with different concentration of tin ion. **Figure 14** showed the graph of electrical resistivity and conductivity against percentage cobalt ions. The decrease in electrical conductivity could be as a result of increase in the thickness of the deposited thin films due to increase in cobalt ion concentration. The decrease in electrical conductivity may also be attributed to low conductivity of cobalt compared to that of copper. Shariffudin *et al*. [60] suggested that increase in electrical resistivity is due to increased trapped carriers in the grains boundaries which may be due to porosity of the deposited films.

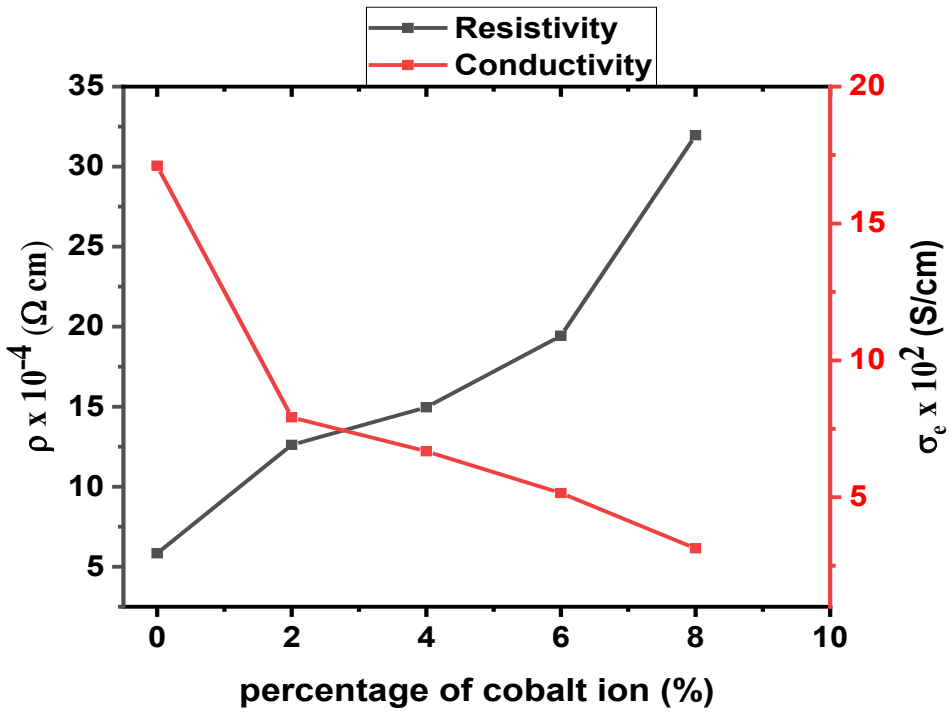

Figure 14 Variation of electrical resistivity and conductivity with percentage of cobalt ion.

Table 4 Electrical properties of cobalt doped copper selenide thin films deposited at different dopant concentration.

Dopant conc.	$V \times 10^{-3}$ (volts)	$I \times 10^{-5}$ (amps)	R (Ω)	Thickness (nm)	R_s (Ω/sq)	$\rho \times 10^{-4}$ $(\Omega\ cm)$	$\sigma_e \times 10^{2}$ (S/cm)
CuSe	1.44	5.43	26.64	48.41	120.69	5.84	17.11
Co: 2 %	4.77	10.88	43.85	63.53	198.65	12.62	7.92
Co: 4 %	30.86	94.96	32.50	101.65	147.21	14.96	6.68
Co: 6 %	3.39	11.24	30.13	142.31	136.50	19.43	5.15
Co: 8 %	4.25	10.65	39.91	176.79	180.77	31.96	3.13

Conclusions

Electrosynthesis of copper selenide and cobalt doped copper selenide thin films has been successfully carried out at room temperature using 3 electrodes setup. Formed CuSe and Co doped CuSe thin films were subjected to optical, structural, morphological, compositional and electrical analyses. Improvements in optical properties of CuSe were observed as cobalt percentage concentration increased from 2 to 8 %. Absorbance values of the films ranged between 0.1 and 0.81 while transmittance values were in the range of 15.59 and 78.68 %. Energy band gap values were found to vary from 2.10 to 2.28 eV. These results showed that cobalt as a dopant could be used to modify properties of copper selenide thin films. Good optical responsiveness of the films was confirmed by values of the reflectance, refractive index, extinction coefficient and optical conductivity. Structural analysis showed that the deposited films are polycrystalline in nature with hexagonal structural phase. Crystallite sizes of range 27.56 and 34.27 nm were obtained while dislocation density lied between 1.59×10^{15} and $1.05 \times 10^{15}\ lines/m^2$. Microstrain ranged between 1.39×10^{-3} and 1.13×10^{-3}. Micrograph images showed flake-like particles that increased in size as percentage of cobalt increased. Energy dispersive spectroscope (EDS) results confirmed the incorporation of cobalt on the deposited copper selenide films. Electrical resistivity of the films increased from 5.84×10^{-4} to $31.96 \times 10^{-4}\ \Omega\ cm$ while conductivity decreased from 17.11×10^{2} to 3.13×10^{2} S/cm. These properties of the deposited thin films positioned them for solar cell and optoelectronics device applications such as light emitting diodes, photodectors, laser diodes and others.

Acknowledgements

We wish to appreciate the contributions made by staff of Nano Research Group of University of Nigeria Nsukka, Enugu state, Nigeria, Electronic Microscopic unit, University of Cape Town, South Africa and National Geosciences Research Laboratories, Nigeria Geological Survey Agency, Kaduna State in analysis of these samples.

References

[1] M Petrovic, M Gilic, J Cirkovic, M Romcevic, N Romcevic, J Trajic and I Yahia. Optical properties of CuSe thin films-band gap determination. *Sci. Sintering* 2017; **49**, 167-74.

[2] AA Yadav. Nanocrystalline copper selenide thin films by chemical spray pyrolysis. *J. Mater. Sci. Mater. Electron.* 2014; **25**, 1251-7.

[3] AL Donne, V Trifiletti and S Binetti. New Earth-Abundant thin film solar cells based on chalcogenides. *Front. Chem.* 2019; **7**, 297.

[4] AA Yadav. Photoelectrochemical studies on spray deposited copper selenide thin films. *J. Mater. Sci. Mater. Electron.* 2014; **25**, 3096-102.

[5] IA Ezenwa, NA Okereke and NL Nonso. Optical properties of copper selenide thin film. *Int. Res. J. Eng. Sci. Tech. Innovat.* 2013; **2**, 82-7.

[6] S Thirumavalavan, K Mani and S Sagadevan. Investigation of the structural, optical and electrical properties of copper selenide thin films. *Mater. Res.* 2015; **18**, 1000-7.

[7] BM Palve, SR Jadkar and HM Pathan. A simple chemical route to synthesize the umangite phase of copper selenide (Cu_3Se_2) thin film at room temperature. *J. Semiconduct.* 2017; **38**, 063003.

[8] R Yousefi. *Metal-Selenide nanostructures: Growth and properties. In*: A Qurashi (Ed.). Metal Chalcogenide Nanostructures for Renewable Energy Applications. Scrivener Publishing LLC, Beverly, Massachusetts. 2014.

[9] HK Sadekar. Optical and structural properties of cuse thin films deposited by chemical bath deposition (CBD) technique. *Int. Res. J. Sci. Eng.* 2018; **2018**, 20-2.

[10] A Zyoud, K Murtada, H Kwon, HJ Choi, TW Kim, MHS Helal, M Faroun, H Bsharat, D Park and HS Hilal. Copper selenide film electrodes prepared by combined electrochemical/chemical bath depositions with high photo-electrochemical conversion efficiency and stability. *Solid State Sci.* 2018; **75**, 53-62.

[11] SS Dhasade, JV Thombare, RS Gaikwad, SV Gaikwad, SS Kumbhare and S Patil. Copper selenide nanorods grown at room temperature by electrodeposition. *Mater. Sci. Semicond. Process.* 2015; **30**, 48-55.

[12] RS Mane, AV Shaikh, OS Joo, SH Han and HM Pathan. Electrodeposition of copper selenide films from acidic bath and their properties. *AIP Conf. Proc.*2012; **1451**, 194.

[13] B Güzeldir and M Sağlam. Using different chemical methods for deposition of copper selenide thin films and comparison of their characterization. *Spectrochim. Acta Mol. Biomol. Spectros.* 2015; **150**, 111-9.
[14] Z Lin, C Hollar, JS Kang, A Yin, Y Wang, HY Shiu, Y Huang, Y Hu, Y Zhang and XA Duan. Solution processable high-performance thermoelectric copper selenide thin film. *Adv. Mater.* 2017; **29**, 1606662.
[15] A Astam, Y Akaltun and M Yıldırım. Conversion of SILAR deposited Cu3Se2 thin films to $Cu_{2-x}Se$ by annealing. *Mater. Lett.* 2016; **166**, 9-11.
[16] ST Pawar, GT Chavan, VM Prakshale, A Sikora, SM Pawar, SS Kamble, NB Chaure, NN Maldar and LP Deshmukh. Solution grown ZnSe: Co nanocrystalline thin films: The characteristic properties. *AIP Conf. Proc.* 2018; **1989**, 020036.
[17] P Mallikarjuna, J Sivasankar, MR Begam, NM Rao, S Kaleemulla and J Subrahmanyam. Structural, optical and magnetic properties of Co doped ZnSe powders. *Mech. Mater. Sci. Eng. J.* 2017; **9**, 242-8.
[18] J Singh and NK Verma. Structural, optical and magnetic properties of cobalt-doped CdSe nanoparticles. *Bull. Mater. Sci.* 2014; **37,** 541-7.
[19] MA Ashoush, MM El-Okr and ZMA El-Fattah. Preparation of cobalt doped Bi_2Se_3 nano-topological insulators. *J. Mater. Sci. Mater. Electron.* 2017; **28**, 3659-63.
[20] F Ming, H Liang, H Shi, X Xu, G Mei and Z Wang. MOF-derived Co-doped nickel selenide/C electrocatalysts supported on Ni foam for overall water splitting. *J. Mat. Chem. A* 2016; **4**, 15148-55.
[21] J Song, SS Li, S Yoon, WK Kim, J Kim, J Chen, V Craciun, TJ Anderson, OD Crisalle and F Ren. Growth and characterization of CdZnS thin film buffer layers by chemical bath deposition. *In*: Proceedings of the Conference Record of the Thirty-first IEEE Photovoltaic Specialists Conference, Florida. 2005, p. 449-52.
[22] F Göde and S Ünlü. Nickel doping effect on the structural and optical properties of indium sulfide thin films by SILAR. *Open Chem.* 2018; **16**, 757-62.
[23] P Chaudhary and V Kumar. Preparation of ZnO thin film using sol-gel dip-coating technique and their characterization for optoelectronic applications. *World Sci. News* 2019; **121**, 59-66.
[24] D Shelke, P Chaudhari and S Bhusal. Study the rate of deposition of zinc metal ions on metal by using various chemicals. *London J. Eng. Res.* 2019; **19**, 73-80.
[25] S Kumar, S Pande and P Verma. Factor effecting electro-deposition process. *Int. J. Curr. Eng. Tech.* 2015; **5**, 700-4.
[26] K Ravindranah, KDV Prasad and MC Rao. Spectroscopic and luminescent properties of Co^{2+} doped tin oxide thin film by spray pyrolysis. *AIMS Mater. Sci.* 2016; **3**, 796-807.
[27] CC Okorieimoh, U Chime, AC Nkele, AC Nwanya, IG Madiba, AKH Bashir, S Botha, PU Asogwa, M Maaza and FI Ezema. Room-temperature synthesis and optical properties of nanostructured Ba-Doped ZnO thin films. *Superlattice. Microst.* 2019; **130**, 321-31.
[28] M Anbarasi, VS Nagarethinam, R Baskaran and V Narasimman. Studies on the structural, morphological and optoelectrical properties of spray deposited CdS:Pb thin films. *Pac. Sci. Rev. A Nat. Sci. Eng.* 2016; **18**, 72-7.
[29] A Hadri, C Nassiri, FZ Chafi, M Loghmarti and A Mzerd. Effect of acetic acid adding on structural, optical and electrical properties of sprayed ZnO thin films. *Energy Environ. Focus* 2015; **4**, 12-7.
[30] C Awada, GM Whyte, PO Offor, FU Whyte, MB Kanoun, S Goumri-Said, A Alshoaibi, ABC Ekwealor, M Maaza and FI Ezema. Synthesis and studies of electrodeposited yttrium arsenic selenide nanofilms for Opto-Electonic applications. *Nanomaterials* 2020; **10**, 1557.
[31] PP Hankare, AS Khomane, PA Chate, KC Rathod and KM Garadkar. Preparation of copper selenide thin films by simple chemical route at low temperature and their characterization. *J. Alloy. Comp.* 2009; **469**, 478-82.
[32] J Kaur, A Parmar, SK Tripathi and N Goyal. Optical study of $Ge_1Sb_2Te_4$ and GeSbTe thin films. *Mater. Res. Express* 2019, **6**, 046417.
[33] NJ Egwunyenga, NL Ezenwaka, IA Ezenwa and NL Okoli. Effect of annealing temperature on the optical properties of electrodeposited ZnO/MgO superlattice. *Mater. Res. Express* 2019; **6**, 105921.
[34] C Augustine, MN Nnabuchi, RA Chikwenze, FNC Anyaegbunam, PN Kalu, BJ Robert, CN Nwosu, CO Dike and E Taddy. Comparative investigation of some selected properties of Mn_3O_4/PbS and CuO/PbS composites thin films. *Mater. Res. Express* 2019; **6**, 066416.
[35] E Güneri. The Role of Au Doping on the Structural and Optical Properties of Cu_2O Films. *J. Nano Res.* 2019; **58**, 49-67.

[36] R Bekkari, B Jaber, H Labrim, M Quafi, N Zayyoun and L Laahab. Effect of solvents and stabilizer molar ratio on the growth orientation of sol-gel derived ZnO THin films. *Int. J. Photoenergy* 2019; **2019**, 3164043.
[37] AA Abouda, A Mukherjeeb, N Revaprasaduc and AN Mohamed. The effect of Cu-doping on CdS thin films deposited by the spray pyrolysis technique. *J. Mater. Res. Tech*. 2019; **8**, 2021-30.
[38] F Aydın, FM Tezel and 1A Kariper. Optical, electrical, structural and magnetic properties of BiSe thin films produced by CBD on different substrates for optoelectronics applications. *Mater. Res. Express* 2018; **6**, 016425.
[39] P Sreedev, V Rakhesh and NS Roshina. Optical characterization of ZnO thin films prepared by chemical bath deposition method. *IOP Conf. Mater. Sci. Eng.* 2018; **377**, 012086.
[40] E Guneri and A Kariper. Characterization of high quality Chalcogenide thin films fabricated by Chemical Bath Deposition. *Electron. Mater. Lett.* 2013; **9**, 13-7.
[41] 1A Kariper. Synthesis and characterization of CrSe thin film produced via chemical bath deposition. *Opt. Rev.* 2017; **24**, 139-46.
[42] S Mushtaq, B Ismail, M Raheel and A Zeb. Nickel antimony sulphide thin films for solar cell application: Study of optical constants. *Nat. Sci.* 2016; **8**, 33-40.
[43] AA Hssi, L Atourki, N Labchir, M Ouafi, K Abouabassi, A Elfanaoui, A Ihlal and K Bouabid. Optical and dielectric properties of electrochemically deposited p-Cu_2O films. *Mater. Res. Express* 2020; **7**, 016424.
[44] GM Whyte, C Awada, PO Offor, FU Whyte, MB Kanoun, S Goumri-Said, A Alshoaibi, ABC Ekwealor, M Maaza and FI Ezema. Experimental and theoretical studies of the solid-state performance of electrodeposited Yb_2O_3/As_2Se_3 nanocomposite films. *J. Alloy. Comp.* 2021; **855**, 157324.
[45] J Tauc, R Grigorovici and A Vancu. Optical properties and electronic structure of amorphous germanium. *Phys. Status Solidi B* 1966; **15**, 627-37.
[46] LN Ezenwaka, NS Umeokwonna and NL Okoli. Optical, structural, morphological, and compositional properties of cobalt doped tin oxide (CTO) thin films deposited by modified chemical bath method in alkaline medium. *Ceram. Int.* 2020; **46**, 6318-25.
[47] G Nam, H Yoon, B Kim, L Dong-Yul, JS Kim, L Jae-Young. Effect of Co doping concentration on the structural properties and optical parameters of Co-doped ZnO thin films by Sol-Gel dip coating method. *J. Nanoscience Nanotechnology* 2014; **14**, 8544-8.
[48] R Sahebi, MR Roknabadi and M Behdani. Effect of Ag-doping on the structural, optical, electrical and photovoltaic properties of thermally evaporated cadmium selenide thin films. *Mater. Res. Express* 2020; **6**, 126453.
[49] G Poongodi, P Anandan, RM Kumar and R Jayavel. Studies on visible light photocatalytic and antibacterial activities of nanostructured cobalt doped ZnO thin films prepared by sol-gel spin coating method. *Spectrochim. Acta Mol. Biomol. Spectros.* 2015; **148**, 237-43.
[50] M Liu, L Hu, Y Ma, M Feng, S Xu and H Li. Effect of Pt doping on the preferred orientation enhancement in $FeCo/SiO_2$ nanocomposite films. *Sci. Rep.* 2019; **9**, 10670.
[51] E Yücel and Y Yücel. Fabrication and characterization of Sr-doped PbS thin films grown by CBD. *Ceram. Int.* 2017; **43**, 407-13.
[52] EM Mkawi, K Ibrahim, MKM Ali, MA Farrukh and AS Mohamed. The effect of dopant concentration on properties of transparent conducting Al-doped ZnO thin films for efficient Cu_2ZnSnS_4 thin-film solar cells prepared by electrodeposition method. *Appl. Nanoscience* 2015; **5**, 993-1001.
[53] MY Li, M Yang, E Vargas, K Neff, A Vanli and R Liang. Analysis of variance on thickness and electrical conductivity measurements of carbon nanotube thin films. *Meas. Sci. Tech.* 2016; **27**, 095004.
[54] RS Waremra and P Betaubun. Analysis of Electrical Properties Using the four point Probe Method. *In*: Proceedings of the 3rd International Conference on Energy, Environmental and Information System, Semarang, Indonesia. 2018, p. 13019.
[55] A Mb, M Shahryari and S Nanekarany. Study and calculation electrical properties of silver thin layers by four-point probe method. *J. Laser. Optic. Photon*. 2017; **4**, 1000150.
[56] F Cemin, D Lundin, D Cammilleri, T Maroutian, P Lecoeur and T Minea. Low electrical resistivity in thin and ultrathin copper layers grown by high power impulse magnetron sputtering. *J. Vac. Sci. Tech.* 2016; **34**, 051506.
[57] IA Ezenwa, NA Okereke and NL Okoli. Electrical properties of copper selenide thin films. *IPASJ Int. J. Electr. Eng.* 2013; **1**, 1-4.

[58] JYC Liew, Z Talib, W Mahmood, M Yunus, Z Zainal, S Halim, M Moksin, W Yusoff and KP Lim. Structural, morphology and electrical properties of layered copper selenide thin films. *Cent. Eur. J. Phys.* 2009; **7**, 379-84.

[59] PPJ Helan, K Mohanraj and G Sivakumar. Doping of Sn transition metal in $CuSe_2$ thin films and its effect on structural evolvement and opto-electrical properties. *Appl. Phys. Mater. Sci. Process.* 2016; **122**, 718.

[60] SS Shariffudin, M Salina, SH Herman and M Rusop. Effect of film thickness on structural, electrical and optical properties of sol - gel deposited layer by layer ZnO nanoparticles. *Trans. Electr. Electron. Mater.* 2012; **13**, 102-5.